

Protein–Protein Interactions Studied by EPR Relaxation Measurements: Cytochrome *c* and Cytochrome *c* Oxidase

Sevdalina Lyubenova,^{†,§,||} M. Khalid Siddiqui,^{†,||} Marloes J. M. Penning de Vries,^{†,§,||} Bernd Ludwig,^{†,||} and Thomas F. Prisner^{*,†,§,||}

Institute of Physical and Theoretical Chemistry, Institute of Biochemistry, Center for Biomolecular Magnetic Resonance, and Center of Excellence "Macromolecular Complexes", Johann Wolfgang Goethe University, Frankfurt am Main, Germany

Received: September 6, 2006; In Final Form: December 18, 2006

The complex formed between cytochrome *c* oxidase from *Paracoccus denitrificans* and its electron-transfer partner cytochrome *c* has been studied by multi-frequency pulse electron paramagnetic resonance spectroscopy. The dipolar relaxation of a fast-relaxing paramagnetic center induced on a more slowly relaxing center can be used to measure their distance in the range of 1–4 nm. This method has been used here for the first time to study transient protein–protein complex formation, employing soluble fragments for both interacting species. We observed significantly enhanced transversal relaxation of the Cu_A center in cytochrome *c* oxidase due to the fast-relaxing iron of cytochrome *c* upon complex formation. The possibility to measure cytochrome *c* oxidase in the presence and absence of cytochrome *c* permitted us to separate the dipolar relaxation from other relaxation contributions. This allowed a quantitative simulation and interpretation of the relaxation data. The specific temperature dependence of the dipolar relaxation together with the high orientational selectivity achieved at high magnetic field values may provide detailed information on distance and relative orientation of the two proteins with respect to each other in the complex. Our experimental results cannot be explained by any single well-defined structure of the complex of cytochrome *c* oxidase with cytochrome *c*, but rather suggest that a broad distribution in distances and relative orientations between the two proteins exist within this complex.

Introduction

Protein–protein interactions are important in a large variety of biological processes such as photosynthesis, respiration, and signal transduction. The formation of protein–protein complexes is essential for redox processes in the mitochondrial and bacterial respiratory chain, where the transfer of electrons is coupled to translocation of protons across the membrane generating an electrochemical proton gradient used for ATP synthesis.^{1–3} In electron transfer interactions, the binding of the electron carriers has to be both specific and transient in order to ensure catalytic efficiency and high turnover. Because of their transient nature, redox complexes are difficult to study and only a small number of structures has been determined so far by X-ray and NMR spectroscopy (e.g., refs 4–7). Computational docking studies have been employed to obtain more information about the structure of protein–protein complexes (e.g., refs 8–10).

Cytochrome *c* oxidase (CcO, complex IV) and cytochrome *c*₅₅₂ (from here on referred to as *c*₅₅₂) are two membrane proteins involved in the respiratory electron transport chain of *Paracoccus denitrificans*. CcO is the terminal enzyme of the respiratory chain and catalyzes the four-electron reduction of oxygen to water.¹¹ The membrane-anchored protein *c*₅₅₂ is the electron donor for this reaction in this bacterium as it shuttles electrons between complex III (cytochrome bc₁ complex) and complex IV.¹² The first electron acceptor in CcO is the binuclear copper center Cu_A, located in subunit II.¹¹ Although the

structures of CcO and *c*₅₅₂ from *P. denitrificans* have been solved,^{13–16} no structure of their complex has been obtained up to now.

The complex of *c*₅₅₂ with CcO is of transient nature, based mainly on electrostatic interactions. Extensive mutagenesis studies have been carried out in order to identify the docking site on CcO.¹⁷ A set of surface exposed acidic residues around the binuclear Cu_A center has been found to play a crucial role in protein binding. Mutagenesis studies, kinetic studies, as well as NMR experiments on the redox partner *c*₅₅₂ have shown that positively charged amino acid residues around the heme cleft constitute the complementary binding site.^{17–19} Computational docking studies for the electron-transfer complexes between CcO and *c*₅₅₂ or horse heart cytochrome *c* (from here on referred to as *c*_{hh}) have been performed, and binding models have been proposed on the basis of these results.^{8–10}

Pulse EPR methods, like pulsed electron–electron double resonance (PELDOR),²⁰ double quantum coherence (DQC),²¹ and relaxation measurements,²² are well-established techniques to measure distances between two paramagnetic centers in the range of 10–70 Å. All of them use the magnetic dipole–dipole coupling between the paramagnetic centers to determine the distance between them. Whereas PELDOR and DQC experiments have been used mainly on nitroxide spin labels and other slowly relaxing paramagnetic centers, relaxation experiments have been applied to obtain distances between a fast relaxing spin (e.g., a metal ion) and a more slowly relaxing spin, as for example nitroxide spin labels or transition metal ions.^{22–26}

Both paramagnetic centers involved in this study have been characterized thoroughly by EPR spectroscopy in the past. The binuclear Cu_A center of different bacterial and mitochondrial

* Corresponding author. E-mail: prisner@epr.uni-frankfurt.de.

[†] Institute of Physical and Theoretical Chemistry.

[‡] Institute of Biochemistry.

[§] Center for Biomolecular Magnetic Resonance.

^{||} Center for Excellence "Macromolecular Complexes."

CcO and of the Cu_A-containing soluble fragment of subunit II (from here on referred to as CcO_{II}) exhibits an EPR spectrum typical for a mixed-valence [Cu^{1.5+}...Cu^{1.5+}] $S = 1/2$ binuclear copper with g -tensor values $g_{xx} = 1.99$, $g_{yy} = 2.02$, and $g_{zz} = 2.18$.^{27,28} Mitochondrial cytochrome *c* shows a rhombic g -tensor with values $g_{xx} = 1.25$, $g_{yy} = 2.26$, and $g_{zz} = 3.06$, typical for biological class I low spin ($S = 1/2$) ferricytochrome.²⁹ The electron spin–lattice relaxation times T_1 of Cu_A in CcO and of mitochondrial cytochrome *c* in the temperature range of 1.5–15 K have been measured.³⁰

Here, we apply X-band (9 GHz) and G-band (180 GHz) pulse EPR spectroscopy to investigate the magnetic dipole–dipole interaction between the cytochrome low-spin Fe³⁺ and the binuclear Cu_A center from CcO in the CcO_{II}:cytochrome *c* protein–protein complex. Stoichiometric 1:1 complex formation is observed in mixtures of the two proteins as a significant enhancement of the transversal relaxation rate of the slowly relaxing Cu_A spin by the fast-relaxing Fe³⁺ spin in the complex. The specific temperature dependence of the dipolar relaxation and high orientational resolution obtained at G-band frequency provide information about the distribution of distances and relative orientations of the two proteins in the complex.

Theory

Dipolar Interaction. Two spins in a magnetic field sense each other through a magnetic dipole–dipole interaction.³¹ The strength of this interaction depends on the distance R between the spins and on the orientation of the vector \vec{R} connecting them with respect to the two magnetic moments:

$$H_{\text{dd}} = \frac{\vec{\mu}_A \cdot \vec{\mu}_B}{R^3} - \frac{3(\vec{R} \cdot \vec{\mu}_A)(\vec{R} \cdot \vec{\mu}_B)}{R^5} \quad (1)$$

In magnetic resonance with an external magnetic field in the z -direction, this Hamilton operator can be expressed as

$$H_{\text{dd}} = \frac{g_A g_B \beta_e^2}{R^3} (A + B + C + D + E + F) \quad (2)$$

where g_A and g_B are the orientation dependent effective g -values of spins A and B, respectively. The secular term A of this Hamiltonian is given by

$$A = (1 - 3 \cos^2(\theta_D)) S_Z^A S_Z^B \quad (3)$$

θ_D is the angle between the external magnetic field and the dipolar vector; S_Z^A and S_Z^B are the respective spin operators. Therefore, the dipolar splitting (2Δ) of the resonance lines of spins A and B is orientation dependent, as will be explained in more detail later on.

Dipolar Relaxation. For two unlike coupled spins, of which one relaxes much faster than the other, dipolar coupling may manifest itself as a change in the relaxation behavior of the slower relaxing spin. From time-dependent perturbation theory, it can be shown that a local minimum in the longitudinal relaxation time T_1 of the slow-relaxing spin (spin A) occurs when the relaxation rate $K = 1/T_1^B$ of the fast-relaxing spin B equals the Larmor frequency of spin A.³² Similarly, a minimum in the transversal relaxation time of spin A can be found when the relaxation rate K is equal to the dipolar coupling strength Δ in angular frequency units. For the two paramagnetic centers investigated here, only the second process will be effective in the accessible temperature range (5–30 K).

Relaxation Measurements. Relaxation measurements were performed with a two pulse Hahn echo sequence ($\pi/2$ -pulse, delay time τ , π -pulse, delay time τ , echo signal). The relaxation behavior caused by dipolar coupling has been calculated to be³³

$$\Phi_{\text{dd}}(2\tau) = C^{-2} \left[\frac{K}{2} ((K + C)e^{-(K-C)2\tau} + (K - C)e^{-(K+C)2\tau}) - \Delta^2 e^{-K2\tau} \right] \quad (4)$$

with $C^2 = K^2 - \Delta^2$.

In the slow-relaxing ($K \ll \Delta$) and the fast-relaxing limit ($K \gg \Delta$), eq 3 reduces to simple monoexponential decay curves:

$$\Phi_{\text{dd}}(2\tau) = \exp\left(\frac{-2\tau}{T_1^B}\right) \quad (5)$$

and

$$\Phi_{\text{dd}}(2\tau) = \exp(-\Delta^2 T_1^B \tau) \quad (6)$$

respectively.

As T_1^B depends strongly on temperature,³⁰ the dipolar relaxation traces are also dependent on temperature.

Orientation and Temperature Dependence. The dipolar coupling Δ depends on the angle θ_D of the dipolar vector with respect to the external magnetic field. In an experiment on disordered frozen solution samples, where molecules with many different orientations of the dipolar vector are excited (as in our case at X-band frequencies), the resulting dipolar echo decay is a sum of the decays caused by all excited orientations. This manifests itself in a non-exponential echo decay curve at higher temperatures where the dipolar relaxation is sensitive to Δ (explained in more detail in part A of Supporting Information). This effect is taken into account in our numerical simulations by explicitly including the copper hyperfine coupling and by averaging over all molecular orientations that are in resonance with the chosen microwave frequency within an inhomogeneous line width, which is determined by other unresolved hyperfine interactions.

For spin systems with such large g -anisotropies as cytochrome *c*, the dipolar splitting depends not only on the orientation of the dipolar axis with respect to the external magnetic field but also strongly on the orientation of the cytochrome *c*. Some of the other terms, in particular C and D, also contribute to the dipolar splitting (up to 10%). These effects change the width and shape of the dipolar Pake pattern and have been included in the numerical simulations of our data.

At G-band frequency (180 GHz), the anisotropic g -tensor dominates all other interactions of the Cu_A paramagnetic species by far and leads to a well-resolved powder pattern (see Figure 1b). In this case, depending on spectral position, spins with a much smaller distribution of orientations can be excited, which makes this experiment very sensitive to the orientation of the dipolar vector with respect to the Cu_A g -tensor frame. Different spectral positions within the powder spectrum relax according to their effective dipolar coupling $\Delta(\theta_D)$, resulting in anisotropic relaxation.

Extraction of Dipolar Relaxation Traces. The total echo signal decay is given as the product of an intrinsic signal decay of spin A (which includes its own intrinsic relaxation and electron spin echo envelope modulation (ESEEM) effects) and the dipolar relaxation from spin B:

$$\Phi_{\text{tot}}(2\tau) = \Phi_{\text{Adecay}}(2\tau) \Phi_{\text{Ahf}}(2\tau) \Phi_{\text{dd}}(2\tau) \quad (7)$$

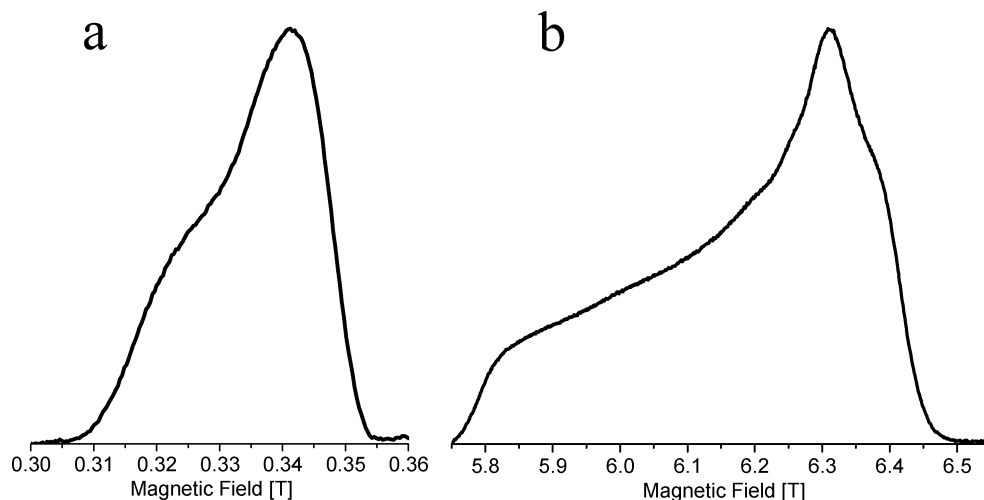


Figure 1. Field-swept echo-detected EPR spectra of the mixed-valence binuclear Cu_A center in CcO_{II} : (a) X-band frequency (9.72 GHz), 100 μM CcO_{II} , $T = 15$ K, pulse separation $\tau = 120$ ns. (b) G-band frequency (180 GHz), 3 mM CcO_{II} , $T = 5$ K, pulse separation $\tau = 300$ ns, main field sweep with a sweep rate of 150 G/min.

where Φ_{Adecay} represents the intrinsic echo decay of spin A alone and Φ_{Ahf} is the ESEEM modulation caused by hyperfine-coupled nuclei to spin A. To obtain the pure dipolar signal decay Φ_{dd} , the total echo decay Φ_{tot} needs to be divided by the signal of spin A alone, which is given by

$$\Phi_A(2\tau) = \Phi_{\text{Adecay}}(2\tau) \Phi_{\text{Ahf}}(2\tau) \quad (8)$$

This division can be easily accomplished experimentally in the case of protein–protein complexes, because Φ_{tot} and Φ_A can be measured independently. The extraction of the pure dipolar relaxation function Φ_{dd} is a prerequisite for a quantitative simulation and interpretation of such relaxation measurements.

Materials and Methods

Sample Preparation. The Cu_A -containing soluble fragment of CcO (CcO_{II}) and the cytochrome c_{552} soluble fragment from *P. denitrificans* have been expressed in a heterologous system in *Escherichia coli* and purified as previously reported.^{12,34} The soluble fragment of cytochrome c_1 was derived from the bc_1 complex, containing 220 amino acid residues expressed in *E. coli*.³⁵ It carries negative surface charges like CcO_{II} and therefore does not interact with CcO_{II} and was used as a negative control in the EPR experiments. Cytochrome c from horse heart (Sigma-Aldrich) was dissolved in 25 mM HEPES-KOH buffer at pH 7.0.

To fully oxidize c_{hh} and c_{552} for EPR experiments, these fragments were incubated with catalytic amounts of cytochrome c oxidase from *P. denitrificans* for 30 min and then purified by gel filtration using a 5 mM HEPES-KOH buffer and 10% glycerol at pH 7.0. Cytochrome c_{hh} , c_{552} , and c_1 concentrations were determined by recording redox difference spectra with extinction coefficients $\Delta\epsilon_{550-535} = 21.0$, $\Delta\epsilon_{551-540} = 19.4$, $\Delta\epsilon_{553-540} = 19.4 \text{ mM}^{-1} \text{ cm}^{-1}$ for c_{hh} , c_{552} , and c_1 , respectively. The CcO_{II} concentration was determined by taking absorption spectra with an extinction coefficient $\epsilon_{480} = 3.0 \text{ mM}^{-1} \text{ cm}^{-1}$.³⁴ The samples used for EPR measurements typically contained 100 μM fully oxidized CcO_{II} and 100 μM fully oxidized cytochrome in 5 mM HEPES-KOH buffer and 10% glycerol at pH 7.0. The samples were transferred into standard quartz EPR tubes and subsequently frozen in liquid nitrogen.

X-Band Pulse EPR Spectroscopy. Electron spin echo decay measurements were performed using a Bruker Elexsys-580 X-band spectrometer equipped with a Bruker MD5–W1 cavity

and an Oxford CF935 helium flow cryostat with ITC-5025 temperature controller. A two-pulse $\pi/2-\tau-\pi$ Hahn echo sequence was used to measure both the field-swept EPR spectra (Figure 1a) and the echo decay traces. The Cu_A center in CcO_{II} exhibits a spectrum as observed in literature before;^{27,28} the bacterial cytochromes have g -tensor values and relaxation rates in the temperature range 5–15 K that are very similar to those observed for mitochondrial cytochrome c .^{29,30}

The two-pulse echo decay experiments were performed in the temperature range 10–25 K and taken at a field position corresponding to the maximum of the Cu_A signal (corresponding to the $g_{xx} = g_{yy} = g_{\perp}$ position). The lengths of the microwave $\pi/2$ - and π -pulses were 20 and 40 ns, respectively, and the shortest value for τ was 120 ns, because of the dead time of the spectrometer. The echo decay traces of the protein mixtures and CcO_{II} alone were taken with exactly the same experimental settings, and both traces were corrected for baseline artifacts by subtraction of off-resonance traces. The echo decay traces were reproducible to a very high accuracy for the same protein concentrations and did not depend on the freezing procedure. The signal amplitude, however, was not so reproducible, and therefore, the echo decay traces were normalized to 1 for the shortest τ value.

G-Band Pulse EPR Spectroscopy. Echo decay measurements were performed on a home-built 6.4 T, 180 GHz pulse EPR spectrometer.^{36,37} A two-pulse echo sequence as described above was used for all measurements, with typical $\pi/2$ -pulse lengths of 35–40 ns and a minimum τ value of 200 ns. The relaxation measurements were mainly performed between the signal maximum and the high-field edge (Figure 1b), corresponding to the g_{yy} and g_{xx} positions, respectively, in a temperature range of 5–15 K. The temperature was measured by a sensor at the sample position with an estimated error of less than 1 K. The superconducting magnet contains a sweep coil with a span of 0.15 T, so in order to obtain the full field-swept spectra of Cu_A (approximately 0.7 T wide) the main coil needed to be swept. This method does not provide us with accurate absolute values of the magnetic field, but calibration with an internal Mn^{2+} standard and simulations indicate that the field sweep is linear within the needed accuracy. Such field-swept spectra were taken with different τ values to look for anisotropy of the dipolar relaxation at high fields. Due to the strongly increased spectral width of the Cu_A spectra at G-band

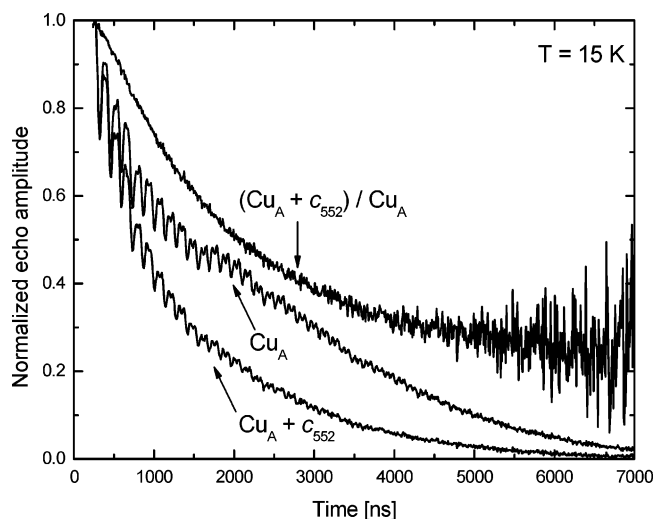


Figure 2. Electron spin echo decay traces of 100 μM CcO_{II} alone (Cu_A) and in a 100 μM :100 μM mixture with c_{552} ($\text{Cu}_A + c_{552}$). The division of these two time traces yields the pure dipolar relaxation trace $(\text{Cu}_A + c_{552})/\text{Cu}_A$. All measurements performed at a magnetic field value of $B_0 = 0.3414$ T, microwave frequency $\nu_{\text{MW}} = 9.72$ GHz, and a temperature of 15 K.

frequency, the typical sample concentration was 200 μM for these measurements.

Analysis of Experimental Data. A home-written MatLab simulation program based on the theory described above has been used to simulate the dipolar relaxation time traces at different temperatures for the protein–protein complex between CcO_{II} and cytochromes. The experimental dipolar relaxation traces at different temperatures were simultaneously fitted via either a SIMPLEX or a sequential quadratic programming algorithm. Fit parameters for a single binding geometry were as follows: the distance between the two paramagnetic centers R ; the polar angles of the dipolar vector with respect to the Cu_A g -tensor frame (θ'_D, φ'_D); the Euler angles (α, β, γ) of the cytochrome g -tensor with respect to the Cu_A g -tensor frame; the exchange coupling J ; and an offset to account for the amount of unbound CcO_{II} . Additionally, the literature values of the cytochrome T_1 relaxation times as a function of temperature were allowed to vary within a factor of 2 to account for experimental errors. The consistency and significance of the obtained fit parameters were tested by repeated fit minimization procedures with arbitrary starting values of the fit parameters. In all cases, the obtained minima were reproduced for many different starting values and are therefore assumed to be global minima.

Results

Extraction of Dipolar Relaxation Traces. In the protein–protein complexes under study, two $S = 1/2$ spins are coupled to each other: the binuclear mixed-valence Cu_A in CcO_{II} as the slowly relaxing observer spin and Fe^{3+} in its low-spin state in cytochrome c as the rapidly relaxing spin. Electron spin echo decay measurements of Cu_A were performed in order to examine the distance and orientation between the redox partners Cu_A in CcO_{II} and Fe^{3+} in cytochrome c , bound in a protein–protein complex. In this experiment, the intensity of the Hahn echo was recorded as a function of the separation time τ between the two pulses. Figure 2 shows the two-pulse echo decay traces of CcO_{II} alone in comparison with the decay of the CcO_{II} and c_{552} mixture measured under the same experimental conditions. The presence of Fe^{3+} caused a significantly faster decay of the echo of Cu_A

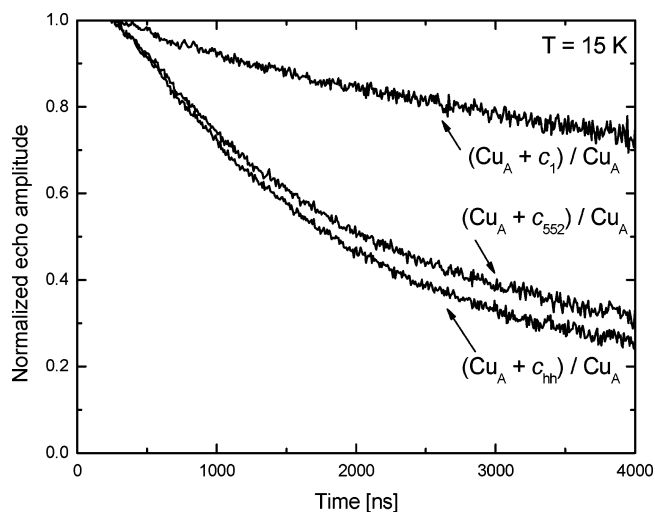


Figure 3. Dipolar relaxation traces of 100 μM :100 μM mixtures of CcO_{II} with c_{1h} ($(\text{Cu}_A + c_{1h})/\text{Cu}_A$), c_{552} ($(\text{Cu}_A + c_{552})/\text{Cu}_A$), and c_1 ($(\text{Cu}_A + c_1)/\text{Cu}_A$) measured with the same experimental parameters as in Figure 2.

due to dipole–dipole interactions between the two paramagnetic centers. As described in the theoretical section and shown in Figure 2, a division of these two time traces removes all intrinsic relaxation and hyperfine modulation of the Cu_A paramagnetic center and allows extraction of the pure dipolar relaxation traces. The division method was applied to all experimental echo decay traces shown further on.

Protein–Protein Complex Formation. The dipole–dipole interaction of Cu_A with the Fe^{3+} of three different cytochromes has been investigated: a soluble fragment of c_{552} , which in the bacterium serves as a membrane-anchored electron donor to CcO ,^{12,17} c_{1h} , which is often used as a substrate in enzymatic assays for the bacterial oxidase, providing high turnover activity,¹⁹ and c_1 , a soluble fragment derived from the *P. denitrificans* cytochrome bc_1 complex, which due to its highly negative surface potential cannot form a complex with CcO_{II} and is used as a negative control.³⁵ The dipolar relaxation traces of Cu_A in CcO_{II} with these three different cytochromes are shown in Figure 3. The dipolar relaxation traces of the mixtures of CcO_{II} with both binding cytochromes c_{1h} and c_{552} are very similar and decay much faster than the trace with the control protein c_1 . This is because the distance between the two paramagnetic centers for the specifically bound protein–protein complexes is much shorter than the average intermolecular distance between randomly distributed paramagnetic centers. The paramagnetic centers in the complexes involving cytochromes c_{552} and c_{1h} must have an interspin distance on the order of 2 nm for electron-transfer reactions to occur,^{7–10,18} whereas non-binding c_1 has a significantly larger average intermolecular distance (approximately 25 nm for a cytochrome concentration of 100 μM). The concentration dependences of the binding and non-binding cytochromes are also very different. A linear concentration dependence of the echo decay function was observed for the non-binding cytochrome c_1 , whereas the other two cytochromes showed a very different behavior, depending on the stoichiometric ratio of CcO_{II} and cytochrome c (see Supporting Information part B).

The relaxation rate calculated for the mixture of the nonbinding c_1 with CcO_{II} is only slightly smaller than the experimentally observed value.³⁸ Altogether, these results are clear evidence for the formation of specific protein–protein complexes between CcO_{II} and either c_{552} or c_{1h} , whereas in the case of c_1 only dipolar interactions of randomly distributed cytochromes were detected.

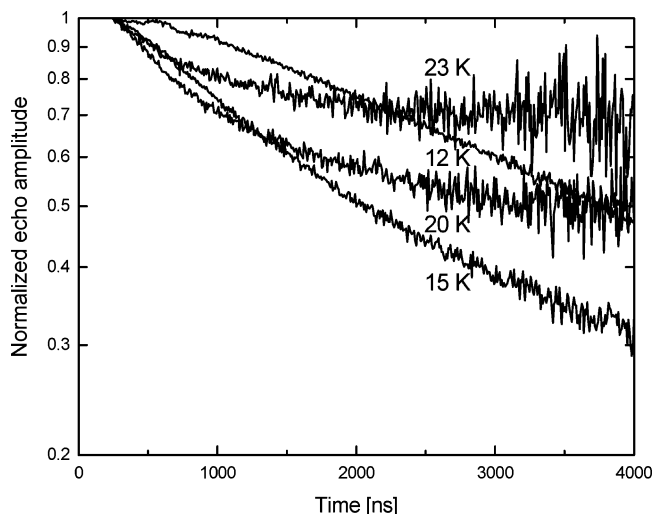


Figure 4. Semilogarithmic plot of the dipolar relaxation traces of 100 μM :100 μM mixture of CcO_{II} with c_{552} , measured at different temperatures as indicated in the plot. Experimental parameters as in Figure 2.

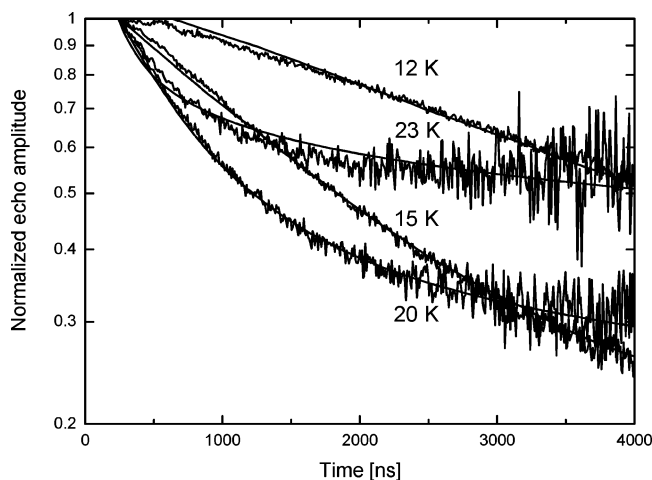


Figure 5. Semilogarithmic plot of the dipolar relaxation traces of 100 μM :100 μM mixtures of CcO_{II} with c_{hh} , measured at different temperatures as indicated in the plot together with simulations (noiseless lines). The fit parameters with the oversimplified model are as follows: dipolar angles, $\vartheta'_D = 54^\circ$, $\varphi'_D = 11^\circ$; distance Fe^{3+} to Cu_A center, $R_1 = 2.3$ nm, $R_2 = 4$ nm; Euler angles, set1 = $(27, 6, 29)^\circ$, set2 = $(90, 57, 12)^\circ$; relative amplitudes of both structures, $A_1 = 1.2$, $A_2 = 1$; unbound $\text{CcO}_{\text{II}} = 11\%$. Experimental parameters as in Figure 2.

Similar results have been obtained at G-band (180 GHz) frequency (data not shown).

In protein samples, aggregation occurs upon freezing if no cryo-protectant, such as glycerol, is added. The addition of 10% glycerol to the protein samples slowed down the dipolar relaxation traces substantially, but no further change in the dipolar relaxation traces was observed by increasing the glycerol content to 20%.

Temperature Dependence of Dipolar Relaxation Traces.

Due to the strong temperature dependence of the T_1 relaxation time of cytochrome c , the dipolar relaxation traces depend strongly on temperature with a minimum in dipolar relaxation time for the condition $1/T_1 = \Delta$. The dipolar relaxation traces in the temperature range 12–23 K of the complex of CcO_{II} with c_{552} are shown in Figure 4 and with c_{hh} in Figure 5. Both complexes exhibit a pronounced minimum in dipolar relaxation (Figures 4 and 5). In accordance with theory, the low-temperature decay trace (12 K) is monoexponential, whereas

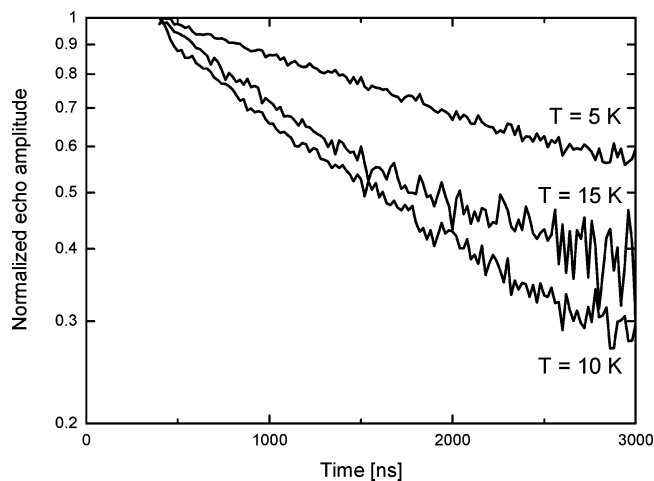


Figure 6. Semilogarithmic plot of the dipolar relaxation traces of 200 μM :200 μM mixture of CcO_{II} with c_{hh} , measured at G-band frequency. The different temperatures are indicated in the plot. All measurements were performed at a magnetic field value of $B_0 = 6.362$ T, microwave frequency $\nu_{\text{MW}} = 180$ GHz.

the higher temperature decay traces show strongly non-exponential behavior due to orientation dependence of the dipolar coupling (see Supporting Information part A). The temperature dependences of the echo decay traces of the complexes with c_{552} and c_{hh} are qualitatively similar but not identical. This probably reflects differences in complex structure as will be discussed later on.

The temperature dependence of the echo decay traces for the c_1 mixture is again very different (data shown in Supporting Information part C). The dipolar relaxation enhancement is much weaker in this case; the decay curves are monoexponential at all temperatures and do not show any pronounced minimum in dipolar relaxation. Again, this is in full agreement with our notion that c_1 does not form a specific protein–protein complex with CcO_{II} .

High-Field Pulsed EPR Measurements. Despite the higher concentration of the protein samples used at G-band (200 μM at G-band, 100 μM at X-band), again a strong temperature dependence was measured for the dipolar relaxation of Cu_A upon mixture with c_{hh} (Figure 6). However, the high-field data could not be fitted with the cytochrome T_1 values from literature, which implies that the T_1 at G-band frequency differs from that at X-band frequency.

Discussion

Specific Protein–Protein Complex Formed. The significant relaxation enhancement of the Cu_A center in CcO_{II} in the presence of c_{552} or c_{hh} observed by our pulse EPR experiments confirms a previous observation by NMR spectroscopy¹⁸ that complex formation between the two fully oxidized proteins takes place despite the fact that no electron is transferred to the oxidized Cu_A center. For both the natural electron donor c_{552} and the non-homologous c_{hh} , a 1:1 complex was formed with approximately 90% yield at low ionic strength, as was seen by comparison of dipolar relaxation traces for different concentrations of cytochrome c (see Supporting Information part B). In contrast to the other two cytochromes, c_1 does not form a complex with CcO_{II} , which was proven by the very different concentration and temperature dependences of the dipolar relaxation for the mixture of CcO_{II} and c_1 .

Extraction of Dipolar Relaxation Traces. The pure dipolar relaxation traces were obtained by measuring CcO_{II} indepen-

dently from the CcO_{II} :cytochrome *c* complex, followed by a division of the two experimental traces. This enabled a much more precise analysis and quantitative numerical simulation of the experimental traces. The fact that the ESEEM modulation vanished by the division confirmed that the electronic structure of Cu_A does not change upon cytochrome *c* binding. This was already indicated by the observation of identical *g*- and hyperfine tensors of Cu_A in the presence and absence of cytochrome *c*.

Temperature Dependence of the Dipolar Relaxation—Low-Temperature Behavior. The monoexponential X-band relaxation traces taken at 12 K of the complexes with c_{hh} and c_{552} could be both simulated very well by the known values of the cytochrome *c* T_1 relaxation times³⁰ as theoretically predicted by eq 5 and not by a correlation time given by the expression $\sqrt{T_1 T_2}$, which was suggested for relaxation studies performed on a spin-labeled myoglobin and a porphyrin–nitroxide model system.^{23,24} This is evidence that the intrinsic relaxation of Cu_A is the same in the CcO_{II} protein whether it is bound to cytochrome *c* or not. The small non-exponential contribution of these experimental decay traces at short τ values arises from overlap of the fast-decaying cytochrome signal still visible at low temperatures.

Temperature Dependence of the Dipolar Relaxation—High-Temperature Behavior. The 23 K data of both complexes show a strongly non-exponential decay with a surprisingly large offset (the dipolar relaxation does not go to zero) of about 50%. Origins of this offset could be that (1) unbound CcO_{II} is present and, hence, Cu_A spins that are unaffected by dipolar relaxation show up as a constant contribution, having no dipolar decay, or (2) there is a contribution of spin pairs whose dipolar angle (θ_D) is approximately the magic angle; see also Supporting Information part A. Both origins could be excluded here because (1) no such contribution from unbound CcO_{II} was observed at lower temperature (12 K), and (2) in a powder sample, it is impossible for 50% of the spin pairs to have θ_D near to the magic angle for any geometry of the protein complex.

Therefore, simultaneous fits of the X-band dipolar decay traces at all temperatures were performed to investigate the protein complex structure. Assuming a single binding geometry of the complex, a number of structures was found with a similar quality of the fit as the one shown in Figure 5. The *R* values of these fit structures range from 1.9 to 2.6 nm and have very specific values of the exchange coupling *J* and dipolar and Euler angles. The fit algorithm had optimized the dipolar coupling distribution in such a way that the low-frequency dipolar coupling distribution of the disordered sample average was almost identical for all these structures and had a sharp and narrow maximum around zero frequency. This feature was necessary to account for the large offset at long τ values by causing very fast dipolar relaxation that had almost fully decayed during the spectrometer dead time. At X-band frequency, the simulated echo decays corresponding to these structures are indistinguishable due to experimental dead time, which allows no values shorter than 120 ns for the pulse separation time τ (see Supporting Information part A).

Orientation Selectivity at G-Band Frequencies. To test if any of these structures describes the protein complex in reality, we performed high-field G-band EPR relaxation measurements. As described before, the possibility to selectively observe molecules with a specific orientation with respect to the magnetic field provides us with more detailed information on the geometry of the complex in disordered frozen solution samples. The different temperature dependence observed at G-band (Figure 6) can be explained by assuming a significant

increase of the relaxation rate of the fast-relaxing cytochrome. The spectrum of cytochrome *c* is, however, too broad to be measured at G-band. An estimate of the cytochrome T_1 at G-band can be made by determining the dipolar relaxation of Cu_A in the presence of c_{hh} at low temperatures where the dipolar relaxation equals the longitudinal relaxation of the fast-relaxing spin (eq 5). From the 5 K measurements, we estimated 2 orders of magnitude faster relaxation rates at G-band frequency for cytochrome *c* (1.6 ms at X-band versus 6 μ s at G-band). Such enhanced relaxation rates at higher frequencies are in agreement with theoretical predictions for the direct and the Raman process, which are the dominant relaxation mechanisms at these temperatures for cytochrome *c*.³⁹ As the T_1 of cytochrome *c* is an important parameter for our quantitative simulations, it is very difficult to extract a reliable value of the dipolar coupling strength by fitting the temperature-dependent relaxation traces at G-band. Nevertheless, it is possible to obtain valuable angular information of the protein complex from the G-band measurements performed at different spectral positions at a temperature where the relaxation enhancement is sensitive to the dipolar coupling Δ (see eq 6). Simulations of all structures from fits of the X-band temperature-dependent relaxation traces showed a pronounced anisotropy of the dipolar relaxation traces at g_{xx} and g_{yy} spectral positions at G-band. However, no differences in dipolar relaxation were observed experimentally in the spectral range between g_{xx} and g_{yy} within the given experimental signal-to-noise ratio. Field-swept echo-detected spectra for different τ values also did not show any indication of strong relaxation anisotropy. On the basis of these experimental results, we discarded all the solutions found by X-band fits assuming a single complex structure.

Two-Site Model for the Protein–Protein Complex. The lack of relaxation anisotropy at G-band can be explained by the existence of several structures with different cytochrome orientations, dipolar angles, and/or distances. To test this hypothesis, a simple model with two distinct binding sites was incorporated in the fitting procedure. This led to more free parameters, but nevertheless, a pronounced minimum was repeatedly found for fits with random starting values. One Fe^{3+} to Cu_A distance was always in the range of 1.8–2.3 nm, and a second long distance was found with approximately 4 nm. The populations of the two sites varied between 1:1 and 2:1. The Euler angles, describing the relative orientations of the molecules in the complex, are not well-defined within this model.

The complex with the short distance causes a strong decay within the dead time of the experiment and is therefore only present in the time traces with a reduced relative intensity (see Supporting Information part A). This component accounts mostly for the large offset of the dipolar relaxation traces at high temperatures. The long distance complex accounts for most of the details of the non-exponential decay curves. Simulations based on this model are in much better agreement with the high-field EPR data. Even for this oversimplified model of just two binding geometries, some of the solutions found by fit-minimalization of the X-band data predict only small relaxation anisotropy at G-band frequency, which is in agreement with our experimental G-band results. Such a fit with the model assuming two complex geometries is overlaid with the experimental traces in Figure 5, and the parameters are given in the figure caption.

The fact that a single complex geometry does not agree with the high-field data may be explained on the one hand by the two-step model for complex formation between electron-transfer proteins proposed previously.^{6,18,40} This model, based on kinetic

studies, NMR data, and MD simulations, suggests that in a first step a rather unspecific encounter complex is formed, which then, in a second step, rearranges to a more specific complex that is optimized for electron transfer. Whereas the first step is guided by electrostatic interactions to achieve high affinity, the formation of the latter is driven by specific van der Waals forces. Hence, cytochromes bound in electron-transfer complexes with a short Cu_A to Fe^{3+} distance and one well-defined geometry, as well as cytochromes bound in encounter complexes (at larger distances) may be present in frozen solution samples.

On the other hand, the protein complex may consist of a dynamic ensemble of conformations with distances in the range of 2–4 nm where an electron is transferred whenever the two redox centers are close enough.^{6,10} Both models are in agreement with our simulations but cannot be distinguished on the basis of our experimental constraints, because we cannot unambiguously determine the distance distribution of the ensemble of complex geometries. For this reason, the values of 2 and 4 nm obtained for our simple two-site model should not be over-interpreted in a quantitative manner, but our data clearly indicate the presence of complexes with distances that are larger than the ones required for direct electron transfer. In a computational docking study that made use of the NMR data of Wienk et al.,¹⁸ various complex geometries were needed to account for all the chemical shift changes observed.¹⁰ Neither the single structures nor the structure distributions proposed by docking studies^{8,10} lead to satisfying fits of our experimental results. In these docking studies, solutions with distances too large for direct electron transfer were discarded, which were, however, important to quantitatively interpret the EPR data.

On this basis, it is rather difficult to interpret the small but significant experimental differences between the relaxation traces of the mixtures with c_{hh} and c_{552} . On the basis of our simulations, the less pronounced temperature dependence of the dipolar relaxation of the complex with c_{552} might point to an even broader distribution of distances and/or orientations of the various complexes in this system. This could result from the more highly charged binding surface of c_{hh} in comparison with c_{552} .^{8,16} The lack of the membrane anchor of c_{552} and the absence of the lipid membrane in our experiments in solution may also lead to a larger distribution in complex geometries.

Conclusions

For the first time, pulse EPR techniques have been used successfully to study the interaction between two electron-transfer proteins. Electron spin echo decay measurements of the paramagnetic Cu_A center in the soluble fragment of subunit II of CcO in complexes with different cytochromes were performed. Binding and non-binding cytochromes could be clearly distinguished. The division method provides pure dipolar relaxation traces that can be quantitatively analyzed to obtain details of the structure of a protein-protein complex, without the necessity of taking into account the intrinsic relaxation properties of the observed paramagnetic species.

In the investigated system, the temperature dependence of the dipolar relaxation traces measured at X-band and the orientation-selective measurements at high frequency together suggest that there is a broad distribution of complex structures with interspin distances of 2–4 nm, rather than there being one single well-defined conformation of the protein-protein complex.

Complementary to the PELDOR method, which works preferentially for nitroxide spin labels with long relaxation times and narrow line widths, the relaxation method can be applied

to spectrally broad paramagnetic centers in coupled spin pairs, where one of the spins relaxes extremely fast. Therefore, dipolar interactions between endogenous metal centers in enzymes can be directly measured. In addition, it is possible to apply this method to protein complexes where more than two paramagnetic centers are involved. Our preliminary echo decay experiments of full-size CcO, which contains a total of four paramagnetic centers, in complex with cytochrome *c*, showed that the division method also in this case removes all contributions from other internal paramagnetic centers in CcO to the Cu_A signal and retains only the dipolar relaxation due to external cytochrome *c*. Extensions to membrane-embedded larger protein complexes and supercomplexes can be envisaged and have been initiated in our laboratory.

Acknowledgment. This project is performed within the collaborative research center Molecular Bioenergetics in Frankfurt, financially supported by the German Research Foundation (DFG SFB-472). M.K.S. is the recipient of an International Max-Planck Research School scholarship. Dr. Axel Weber is acknowledged for performing some early X-band experiments within this project, and Julia Janzon and Hans-Werner Müller for supplying cytochrome c_1 .

Supporting Information Available: Detailed description of temperature and orientation dependence of dipolar relaxation, concentration dependence of dipolar relaxation for CcO_{II} and c_{552} protein mixtures, and temperature dependence of dipolar relaxation for cytochrome c_1 . This material is available free of charge via the Internet at <http://pubs.acs.org>.

References and Notes

- (1) Trumppower, B. L.; Gennis, R. B. *Annu. Rev. Biochem.* **1994**, *63*, 675–716.
- (2) Schultz, B. E.; Chan, S. I. *Annu. Rev. Biophys. Biomol. Struct.* **2001**, *30*, 23–65.
- (3) Hosler, J. P.; Ferguson-Miller, S.; Mills, D. A. *Annu. Rev. Biochem.* **2006**, *75*, 165–187.
- (4) Pelletier, H.; Kraut, J. *Science* **1992**, *258*, 1748–1755.
- (5) Lange, C.; Hunte, C. *Proc. Natl. Acad. Sci. U.S.A.* **2002**, *99*, 2800–2805.
- (6) Prudêncio, M.; Ubbink, M. *J. Molec. Recognit.* **2004**, *17*, 524–539.
- (7) Muresanu, L.; Pristovsek, P.; Löhr, F.; Maneg, O.; Mukrasch, M. D.; Rüterjans, H.; Ludwig, B.; Lücke, C. *J. Biol. Chem.* **2006**, *281*, 14503–14513.
- (8) Flöck, D.; Helms, V. *Proteins* **2002**, *47*, 75–85.
- (9) Roberts, V. A.; Pique, M. E. *J. Biol. Chem.* **1999**, *274*, 38051–38060.
- (10) Bertini, I.; Cavallaro, G.; Rosato, A. *J. Biol. Inorg. Chem.* **2005**, *10*, 613–624.
- (11) Richter, O.-M. H.; Ludwig, B. *Rev. Physiol. Biochem. Pharmacol.* **2003**, *147*, 47–74.
- (12) Reincke, B.; Thöny-Meyer, L.; Dannehl, C.; Odenwald, A.; Aidim, M.; Witt, H.; Rüterjans, H.; Ludwig, B. *Biochim. Biophys. Acta* **1999**, *1411*, 114–120.
- (13) Iwata, S.; Ostermeier, C.; Ludwig, B.; Michel, B. *Nature* **1995**, *376*, 660–669.
- (14) Ostermeier, C.; Harrenga, A.; Ermler, U.; Michel, H. *Proc. Natl. Acad. Sci. U.S.A.* **1997**, *94*, 10547–10553.
- (15) Reincke, B.; Pérez, C.; Pristovsek, P.; Lücke, C.; Ludwig, C.; Löhr, F.; Rogov, V. V.; Ludwig, B.; Rüterjans, H. *Biochemistry* **2001**, *40*, 12312–12320.
- (16) Harrenga, A.; Reincke, B.; Rüterjans, H.; Ludwig, B.; Michel, H. *J. Mol. Biol.* **2000**, *295*, 667–678.
- (17) Maneg, O.; Malatesta, F.; Ludwig, B.; Drosou, V. *Biochim. Biophys. Acta* **2004**, *1655*, 274–281.
- (18) Wienk, H.; Maneg, O.; Lücke, C.; Pristovsek, P.; Löhr, F.; Ludwig, B.; Rüterjans, H. *Biochemistry* **2003**, *42*, 6005–6012.
- (19) Drosou, V.; Reincke, B.; Schneider, M.; Ludwig, B. *Biochemistry* **2002**, *41*, 10629–10634.
- (20) Milov, A. D.; Ponomarev, A. B.; Tsvetkov, Y. D. *Chem. Phys. Lett.* **1984**, *110*, 67–72.
- (21) Borbat, P. P.; Freed, J. H. *Chem. Phys. Lett.* **1999**, *313*, 145–154.

- (22) *Biological Magnetic Resonance*; Berliner, L. J., Eaton, S.S., Eaton, G.R., Eds.; Kluwer Academic/Plenum Publishers: New York, 2000; Vol. 19.
- (23) Rakowsky, M. H.; More, K. M.; Kulikov, A. V.; Eaton, G. R.; Eaton, S. S. *J. Am. Chem. Soc.* **1995**, *117*, 2049–2057.
- (24) Budker, V.; Du, J.-L.; Seiter, M.; Eaton, G. R.; Eaton, S. S. *Biophys. J.* **1995**, *68*, 2531–2542.
- (25) Brudvig, G. W.; Blair, D. F.; Chan, S. I. *J. Biol. Chem.* **1984**, *259* (17), 11001–11009.
- (26) Hirsh, D. J.; Beck, W. F.; Innes, J. B.; Brudvig, G. J. *Biochemistry* **1992**, *31*, 532–541.
- (27) Beinert, H. *Eur. J. Biochem.* **1997**, *245*, 521–532.
- (28) Slutter, C. E.; Gromov, I.; Epel, B.; Pecht, I.; Richards, J. H.; Goldfarb, D. *J. Am. Chem. Soc.* **2001**, *123*, 5325–5336.
- (29) Walker, F. A. *Coord. Chem. Rev.* **1999**, 185–186, 471–534.
- (30) Scholes, C. P.; Janakiraman, R.; Taylor, H.; King, T. E. *Biophys. J.* **1984**, *45*, 1027–1030.
- (31) *Principles of Magnetic Resonance*; Slichter, C. P., Ed.; Springer: Berlin, **1978**; Vol. 1.
- (32) Bloembergen, N.; Purcell, E. M.; Pound, R. V. *Phys. Rev.* **1948**, *73*, 679–712.
- (33) Zhidomirov, G. M.; Salikhov, K. M. *Sov. Phys. JETP* **1969**, *29*, 1037–1040.
- (34) Maneg, O.; Ludwig, B.; Malatesta, F. *J. Biol. Chem.* **2003**, 278, 46734–46740.
- (35) Jazon, J. Personal communication to B. L.
- (36) Rohrer, M.; Brüggmann, O.; Kinzer, B.; Prisner, T. F. *Appl. Magn. Res.* **2001**, *21*, 257–274.
- (37) Hertel, M. M.; Denysenkov, V. P.; Bennati, M.; Prisner, T. F. *Magn. Res. Chem.* **2005**, *43*, 248–255.
- (38) Salikhov, K. M.; Dzuba, S. A.; Raitsimring, A. M. *J. Magn. Reson.* **1981**, *42*, 255–276.
- (39) Prisner, T. *Adv. Magn. Opt. Reson.* **1997**, *20*, 245–299.
- (40) Witt, H.; Malatesta, F.; Nicoletti, F.; Brunori, M.; Ludwig, B. *J. Biol. Chem.* **1998**, *273*, 5132–5136.